Effects of Strain Rate and Temperature on Fracture Strength of Ceramic/Metal Joint Brazed with Ti-Ag-Cu Alloy

Do Won Seo
Department of Mechanical Engineering, Chonbuk National University, Chonju, Chonbuk 561-756, Korea
Jae Kyoo Lim*
The Research Center of Industrial Technology, Engineering Research Institute, Faculty of Mechanical and Aerospace System Engineering, Chonbuk National University, Chonju, Chonbuk 561-756, Korea

Ceramics are significantly used in many industrial applications due to their excellent mechanical and thermal properties such as high temperature strength, low density, high hardness, low thermal expansion, and good corrosion resistive properties, while their disadvantages are brittleness, poor formability and high manufacturing cost. To combine advantages of ceramics with those of metals, they are often used together as one composite component, which necessiates reliable joining methods between metal and ceramic. Direct brazing using an active filler metal has been found to be a reliable and simple technique, producing strong and reliable joints. In this study, the fracture characteristics of Si_3N_4 ceramic joined to ANSI 304L stainless steel with a Ti-Ag-Cu filler and a Cu (0.25-0.3 mm) interlayer are investigated as a function of strain rate and temperature. In order to evaluate a local strain a couple of strain gages are pasted at the ceramic and metal sides near joint interface. As a result the 4-point bending strength and the deflection of interlayer increased at room temperature with increasing strain rate. However bending strength decreased with temperature while deflection of interlayer was almost same. The fracture shapes were classified into three groups ; cracks grow into the metal-brazing filler line, the ceramic-brazing filler line or the ceramic inside.

Key Words : Si_3N_4/ANSI 304L, Four-point Bending, Strain Rate, Elevated Temperature, Fracture Strength, Active Metal Brazing

1. Introduction

Ceramic/metal joining is an important technique to apply ceramics to structural components, while its fracture strength is influenced by residual stress and stress concentration caused by differences between the thermal expansion coefficients and the elastic moduli as well (Kutzer, 1965).

Regarding the joining techniques and material combinations, many experimental studies have been conducted (Iseki and Nicholas, 1979 ; Pabst and Elssner, 1980). And some analytical studies on the thermal and residual stresses have been reported (Hamada et al., 1986 ; Fukumoto et al., 1987). Moreover some experimental studies on the strength of ceramic/metal joint have been made (Kobayashi, 1991). However, studying the effect of strain rate and environmental temperature on the strength of ceramic/metal joint is still needed to make accurate evaluation of it.

* Corresponding Author,
E-mail : jklim@moak.chonbuk.ac.kr
TEL : +82-63-270-2321; **FAX** : +82-63-270-2460
The Research Center of Industrial Technology, Engineering Research Institute, Faculty of Mechanical and Aerospace System Engineering, Chonbuk National University, Chonju, Chonbuk 561-756, Korea.
(Manuscript **Received** December 14, 2001 ; **Revised** June 4, 2002)

In this study, four-point bending tests were conducted on Si_3N_4/ANSI 304L-stainless-steel joint specimens under various strain rates and elevated temperatures. In order to evaluate a local strain, a couple of strain gages were pasted near the joint interfaces at the Si_3N_4 and ANSI 304L sides.

2. Materials and Procedure

2.1 Materials

Pressureless-sintered Si_3N_4 and ANSI 304L austenitic stainless steel were joined by the activation metal vacuum-brazing method. An interlayer of copper sheet and the brazing filler metal of Ti-Ag-Cu were used. The material properties and joining conditions are listed in Tables 1 and 2, respectively.

Table 1 Mechanical properties

	Si_3N_4	ANSI 304L	Cu
E (GPa)	304	196	101
v	0.27	0.30	0.33
$\alpha(\times 10^{-6}/℃)$	3.0	15.0	17.7

E : Young's modulus
v : Posson's ratio
α : thermal expansion coefficient

Table 2 Joining condition

Brazing filler	Ti-Ag-Cu
Temperature	800−850 ℃
Atmosphere	Vacuum, 1.3×10^{-3} Pa
Interlayer	Cu

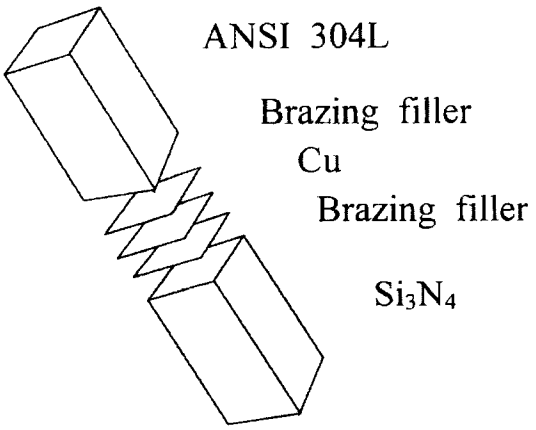

Fig. 1 Specimen configuration

The specification of a test specimen is drawn in Figs. 1 and 2. Si_3N_4 material was cut into $3\times4\times20$ mm bars. The bonding faces of each bar were ground to the average surface roughness of 0.5 μm. The rest faces of the bar were polished with a fine meshed SiC abrasive followed by ultrasonic cleaning with acetone. ANSI 304L bars of the same size with the Si_3N_4 specimens were prepared and the bonding faces were finished with a 1200 grit SiC paper and then macro-etched to remove any oxide films. The thicknesses of a copper interlayer and Ti-Ag-Cu brazing filler are 0.25-0.30 mm and 0.05-0.125 mm, respectively. With the Si_3N_4/ANSI 304L-stainless-steel joint specimens without pre-crack for the four-point bending test shown in Fig. 2, four-point bending test procedures were conducted in accordance with the ASTM standard (ASTM, 1993).

2.2 Experimental procedure

A four-point bending test procedure was performed by a hydraulic universal test machine, Instron model 8516 with 1-ton load cell. The lower span distance was 30 mm and the upper one was 10 mm. A nominal bending strength ignoring the material discontinuity was calculated from the following equation :

$$\sigma_{b4}=3P(L-l)/2wt^2 \quad (1)$$

where P is the maximum load (fracture load), L the lower span, l the upper span, w the specimen width and t the specimen thickness.

Tests were carried out at various cross head speeds (CHS), 0.005, 0.05, 0.5, 5 and 50 mm/min, to evaluate the effect of strain rate on the strength of the joint at room temperature. The effect of environmental temperature was evaluated by tests

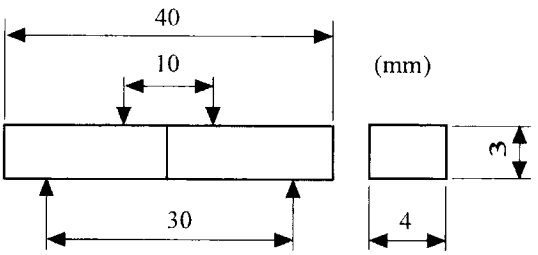

Fig. 2 Dimensions of a 4-point bending specimen

at room temperature (RT), 100, 300 and 500 ℃ at a constant CHS=0.5 mm/min.

In order to evaluate a local strain, a couple of strain gages were pasted near joint interfaces at the Si_3N_4 and ANSI 304L sides. A strain gage of gage length=2 mm was bonded on the lower side where tensile load was applied.

3. Experimental Results and Discussion

3.1 The effect of strain rate

Relationship between bending strength and logarithms of cross head speed, obtained by the four point bending tests at room temperature, is shown in Fig. 3. The linear increase of bending strength over CHS=0.005 mm/min up to CHS= 50 mm/min is in a consistent agreement with other published works for Ti alloy and other metals (Jain et al., 1991 ; Lee and Lin, 1997). The test specimens at room temperature were mainly fractured along the boundary between the Cu interlayer and the metal (ANSI 304L); the cracks initiated at the reaction layer of metal-brazing filler and the fracture behaviour was similar to that in metals.

Variation in deflection at the Cu interlayer, the center of specimen bars, is illustrated in Fig. 4 for various crosshead speeds. The deflection of interlayer at the maximum strength generally increased as increasing a crosshead speed. These result might be influenced by increasing strength with a high loading speed at a relatively high CHS region; the downward deflection of the specimens, increased with an applied load.

Variation in a maximum local strain on a crosshead speed, near the joint interface of the Si_3N_4 and ANSI 304L, is illustrated in Fig. 5, showing strains at maximum strength before fracture. The strain gages were under a applied tensile load, perpendicular to the ceramic/metal interface. The strain value of the metal side remained at a constant with the increase of strain rate, while the local strain of the ceramic side showed a tendency that gradually increased with increasing strain rate. For relatively high strain rates, the gap in strain levels between the Si_3N_4 and ANSI 304L was small. This seems to be due to the high loading speed applied to specimens. The individual deformation seemed to be impossible because two materials were joined with brazing alloy and high loading speed applied. For a relatively low strain rate region, the strain value of Si_3N_4 side was almost zero, but the strain level of ANSI 304L side rose, because of

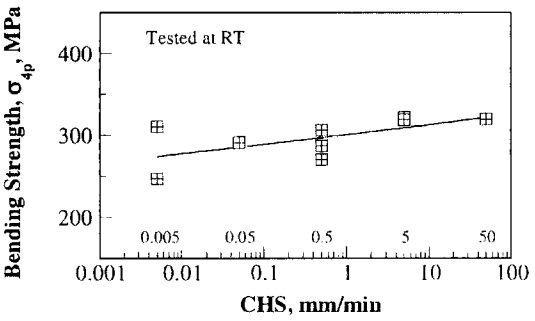

Fig. 3 4-Point bending strength over cross head speeds

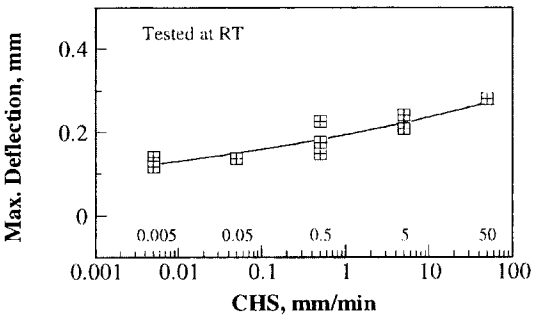

Fig. 4 Maximum displacement over cross head speeds

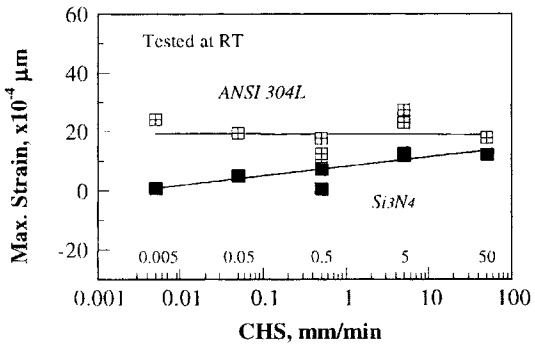

Fig. 5 Maximum stain as a function of cross head speed

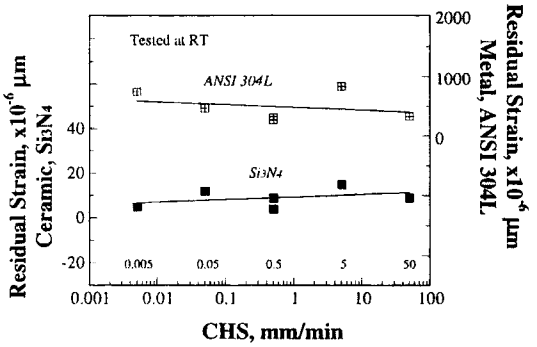

Fig. 6 Residual strain of metal and ceramic as a function of cross head speed

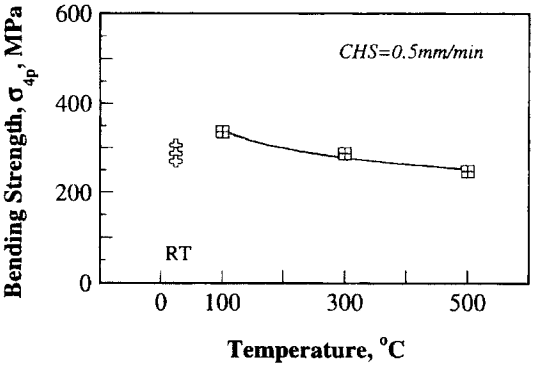

Fig. 7 4-Point bending strength as a function of test temperature

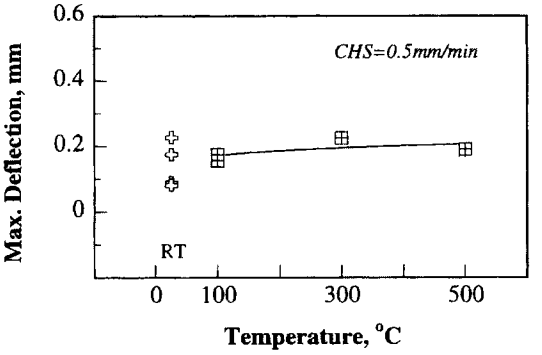

Fig. 8 Maximum displacement as a function of test temperature

the characteristics of the ductile metal.

Figure 6 shows the residual strain of metal and ceramic that remained after fracture with various crosshead speeds. It is seen that the residual strain value of metal is larger than ceramic ; the residual strains of ANSI 304L ranged from 200×10^{-6} to 1000×10^{-6} μm and for Si_3N_4, from 5×10^{-6} to 20×10^{-6} μm. These patterns are typical to metals and ceramics. The gap in residual strain levels between the Si_3N_4 and ANSI 304L gradually decreased with increasing strain rate.

3.2 The effect of environmental temperature

The relations between the bending strength and the test temperature at CHS=0.5 mm/min are shown in Fig. 7. For a high temperature region, from 100 to 500 ℃, the bending strength gradually decreased with increasing test temperature. The specimens at high temperature, were mainly fractured along the interface between the Cu interlayer and the Si_3N_4 ceramic. The cracks initiated at the reaction layer of the ceramic-brazing filler (Ti-reactions). As mentioned above, cracks at room temperature test progressed along the interface between the Cu interlayer and ANSI 304L. But at elevated temperature the weak point changed to Cu/Si_3N_4 interface. It seems that the big difference in thermal expansion coeffcients of Cu metal and Si_3N_4 ceramic makes stress concentration on the Cu/Si_3N_4 interface. The difference of thermal coefficents might increase with increasing temperature and then the stress concentration would increase. So the strength decreased with increasing temperature. The marks as indication RT are for comparison with the strength at room temperature.

The variation of deflection at the Cu interlayer, is illustrated in Fig. 8 under various test temperatures at CHS=0.5 mm/min. At an elevated temperature region, the result shows no significant change in deflection. The values of this curve mean the deflections to fracture. Testing was started after the surrounding temperature was stabilized. In tests the deflection values were measured up to failure. The deflection of the Cu interface affected by heating was eliminated. Thus, the loading deflection level of the Cu interlayer was low.

3.3 The analysis of fracture surface

After failure at room temperature, the Cu

interlayer part was remained on the fracture surfaces of the ceramic side. That is, the joined specimen was mainly fractured along the interface between the Cu interlayer and the metal side (ANSI 304L).

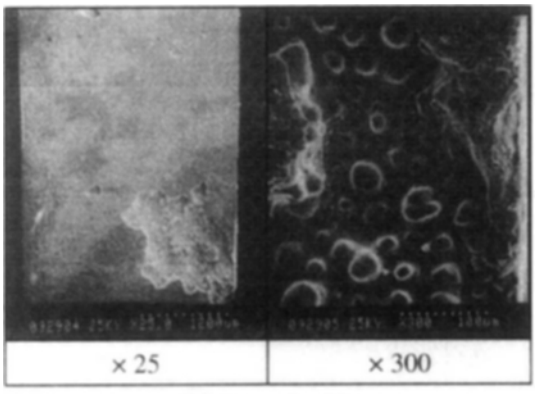

Fig. 9 SEM micrographs of the Cu/ANSI 304L interface at RT test

The SEM photographs for the fracture surface between the Cu interlayer (ceramic side) and the metal side, tested at room temperature, are shown in Fig. 9. Figure 9(a) shows the partially separated brazing filler from the interlayer on the ceramic side. At the right lower side of the figure, we can observe the state of reacted filler. Figure 9 (b) shows the separated brazing filler from the Cu interlayer on the metal side, we can observe the melted condition between the brazing filler and the metal side.

Figure 10 shows the fractured surface between the Cu interlayer (brazing filler) and the ceramic side at a 300 ℃ test. We can observe the brittle behavior in the ceramic joint part at high temperature environment. The crack initiated at the ceramic-brazing filler. But the crack path partially deviated from the interface to the ceramic

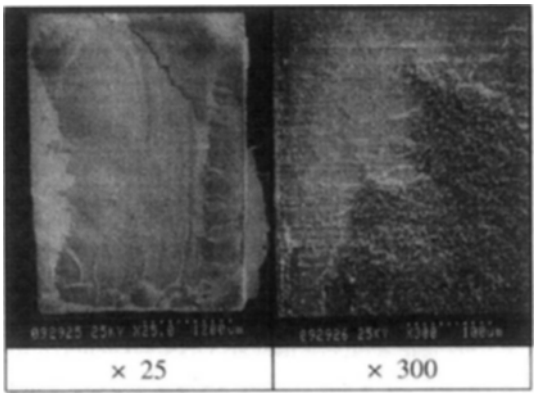

Fig. 10 SEM micrographs of ceramic joint part at 300 ℃

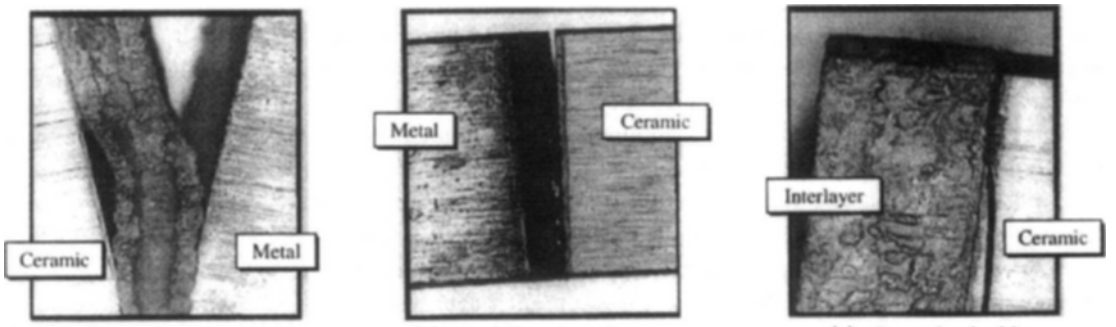

Fig. 11 The classification of fracture shapes

inside and finally resumed its course in the interface.

3.4 The classification of fracture shapes

The fracture shapes are classified into three groups and shown in Fig. 11. When CHS=0.005, 0.5, 5, 50 mm/min at room temperature, the crack initiated at the Cu interlayer/metal interface (Fig. 11(a)). When temperatures are 100 and 500 ℃ (CHS=0.5 mm/min), the crack initiated at the Cu interlayer/ceramics interface (Fig. 11(b)). In the case of 300 ℃ (CHS=0.5 mm/min), the crack initiated at the Cu interlayer/ceramics interface (Fig. 11(c)). Then the crack path changed from the interface to the ceramic inside and it finally resumed its course in the interface.

4. Conclusions

Four-point bending tests were conducted for Si_3N_4/ANSI 304L stainless steel joined specimens with various strain rates and elevated temperatures. The classification of fracture shapes was also performed with the variety of crack path. The results obtained are as follows.

(1) The bending strengths linearly increased with increasing strain rate at room temperature. The cracks initiated at reaction layer of the metal-brazing filler, so the fracture behaviour was similar to that of metals. The downward deflection of Cu interlayer increased with increasing strain rate at room temperature, because of increasing strength with a high loading speed.

(2) With the increase of strain rate at room temperature, the gaps in strain and residual strain levels between the Si_3N_4 and ANSI 304L became gradually smaller, because two materials were joined with brazing alloy and high loading speed applied.

(3) The bending strength decreased with increasing temperature, as the difference in thermal expansion coefficients of two materials increased with temperature.

(4) The cracks grew into the Cu/ANSI 304L interface at room temperature, the Cu/Si_3N_4 interface or the ceramic inside at elevated temperature.

Acknowledgment

The authors wish to express thanks to Professor H. Kobayashi of Tokyo Institute of Technology for the supply of the specimens.

References

ASTM Standards, 1993, "Standard Test Method for Bend Testing of Metallic Flat Materials for Spring Applications Involving Static Loading," *ASTM E 855-90.*

Elsawy, A. H. and Fahmy, M. F., 1998, "Brazing of Si_3N_4 Ceramic to Copper," *J. of Materials Processing Technology*, Vol. 77, pp. 266~272.

Fukumoto, M., Torii, K. and Okane, I., 1987, *Trans. Jpn. Soc. Mech. Eng.*, Ser. C., Vol. 5, No. 496, pp. 2724.

Hamada, K., Kureishi, M., Ueda, M., Enjo, T. and Ikeuchi, K., 1986, *Jpn. J. Weld. Soc.*, Vol. 4, No. 1, pp. 73.

Iseki, T. and Nicholas, M. G., 1979, *J. Mater. Sci.*, Vol. 14, pp. 687.

Jain, M., Chaturvedi, M. C., Richards, N. L. and Good, N. C., 1991, *Mater. Sci. Eng.*, A138, pp. 205~211.

Kobayashi, H., Arai, Y., Nakamura, H. and Sato, T., 1991, *Materials Science and Engineering*, A143, pp. 91~102.

Kutzer, L. G., 1965, *Mater. Des. Eng.*, Vol. 61, pp. 106.

Pabst, R. F. and Elssner, G., 1980, *J. Mater. Sci.*, Vol. 15, pp. 188.

Song, J. H., Lim, J. K. and Takahashi, H., 1996, "Thermal Shock/Fatigue Evaluation of FGM by AE Technique," *KSME Int'l Journal*, Vol. 10, No. 4, pp. 435~442.

Woei-Shyan Lee and Ming-Tong Lin, 1997, "The effects of strain rate and temperature on the compressive deformation behaviour of Ti-6Al-4V alloy," *J. of Materials Processing Technology*, Vol. 71, pp. 235~246.